Solidification of MC SiMn Segregation, Structures and Strength

Eivind G.Hoel* and Johan Kr.Tuset**

*Dept. of Materials Technology, SINTEF, 7034 Trondheim, Norway
Now: Metallurgist, Elkem Mangan Sauda, 4200 Sauda, Norway
**Professor, Dept. of Metallurgy, Norwegian University of Science and Technology, 7034 Trondheim, Norway

Abstract

This presentation focuses on properties and phase compositions of commercial alloys of medium carbon silicomanganese (MC SiMn), and is part of a more comprehensive study of phase relations in the system Mn-Fe-Si-C stating that ternary/quaternary phases of the types $(Mn,Fe)_5SiC$ and $(Mn,Fe)_{17}Si_4C_3$ appear as stable phases in carbon containing alloys [1]. Calculated phase diagrams presented at INFACON 7 [2] for systems where these phases should have been included, need to be revised as a consequence of this.

Commercial MC SiMn is an alloy consisting of 67 - 70% Mn, 17 - 19% Si, and 1.5 - 1.8% C, the rest being approx. 10% Fe and various trace elements. At the temperature of tapping, typically 1500 °C, the liquid metal is close to the coexistance boundary of graphite and SiC. Thus, as the solubility of carbon decreases with temperature, graphite followed by SiC are the first phases to precipitate as the metal is cooled off prior to casting. Solidification of the metal itself takes place below approx. 1260 °C, where the dissolved carbon has dropped to ~0.7% C [3]. The primary phase to form is Me_5Si_3 (23.5% Si), which has a limited solubility of carbon, possibly up to $Me_5Si_3C_{0.22}$ (0.73% C) [4]. Below approx. 1090 °C, the secondary phase $Me_{17}Si_4C_3$ (10.4% Si, 3.33% C) starts to co-precipitate with the first. At approx. 1020 °C the remaining melt solidifies in a eutecticum giving a third compound, Me_3Si (14.6% Si). This phase may transform in the solid state to Me_5Si_2 (17.0% Si) at the temperature of approx. 850 °C. In the final metal the three phases count for approx. 70, 25 and 5%, respectively.

In commercial production of SiMn the metal is casted at a temperature well above the solidus, e.g. 1350 - 1450 °C, which gives delayed cooling and solidification. This in turn has the two negative effects of macro segregation and growth of large grains of the primary phase, Me_5Si_3. Macro segregation results in increased contents of C, Si, Ti and S, in addition to elements from slag inclusions, in the upper 1/4 - 1/3 of the casted metal. In this top layer a number of carbon-based particles and oxide inclusions are found: SiC, TiC, graphite, MnO, MnS, SiO_2, etc. The carbon-based particles are in the top layer concentrated to approx. 5% by weight, which gives an average of approx. 1.5% for the full cast.

Introduction

Commercial production of (ferro)silicomanganese, (Fe)SiMn, is a pyrometallurgical process in which manganese and silicon oxides are carbothermically reduced to metal in a liquid state. The smelting takes place in electric submerged arc furnaces with a load of 15 - 40 MVA, giving a production of 80 - 220 M.T./day at a power consumption of about 4.5 MWh/M.T. In addition, the process produces large amounts of slag, usually 10 - 1500 kg/M.T. of SiMn. The furnace is tapped discontinuously, every 2 - 3 hours, giving tap sizes of 10 - 30 M.T. of metal and proportional amounts of slag. With mixed tapping of slag and metal from one taphole, the separation of the two phases must take place outside the furnace, either by use of a skimmer in the runner or by cascade tapping in ladles. Any slag remaining in the metal ladle may subsequently be removed, by tilting the ladle and dragging off the slag manually or with a mechanical rake.

At the time of casting the ladle is emptied, either by pouring the metal over the ladle lip or through a bottom gate. The first method is 'quick and dirty', the flow rate is high and not easily controlled, and what is present of floating oxides and carbides enter the cast. The ladle can be emptied, however, in a few minutes, or abrupted and restarted at any time. Bottom pouring is in many respects the opposite, the flow rate is lower and can be controlled by throttling the gate, which can be closed and even reopened. Unwanted contents of oxides and carbides are prevented from entering the casted metal, as the inclusions, due to lower density than the metal, float in the opposite direction of the downward metal stream.

The traditional methods are (multi) layer casting or casting in sand moulds, which includes simple equipment that is easy to use with low investment and operating costs, and have a very low down time. Other methods are chill casting and conveyor belt casters, which include more sophisticated equipment with higher investment and operating costs. However, they offer faster cooling and even and thinner casts, which is beneficial to the strength of the metal.

Experimental Work

Synthesized Samples

Commercial SiMn is a mixture of several phases. In order to identify and characterize these phases, a series of samples containing Mn and Si, plus Fe and C when required, were prepared from pure raw materials in alumina crucibles. After melting under inert atmosphere these samples were cooled to sub-solidus temperature for homogenization before they where quenched and subsequently subjected to micro- and x-ray analysis. Thus, the synthesized samples provided the x-ray diffractograms needed for the identification of phases present in the commercial samples, and were also used for micro hardness testing of identical phases appearing in MC SiMn.

Commercial Samples

Three series of industrial castings were carried out at the smelting plant of Elkem Mangan PEA: one chill casting series in iron moulds and two layer casting series in sand beds. In order to vary the cooling rate, the metal was casted with variable thickness in the chill casting series and two different thicknesses in the two layer casting series. Throughout all tests the temperature was measured by means of thermocouples placed in various positions in the castings (PtRh10-Pt t/c), and in selected positions in the mould (NiCr-NiAl t/c) for the chill castings. The thermocouples were connected to a data logger, which recorded the temperature every tenth second.

Chill casting was done in a series of five tests, where the metal was casted in an iron mould, with dimensions 2 x 2 x 0.1 m. To protect the mould the bottom was covered by a 0.5 - 1 cm layer of SiMn-fines. Layer casting was done in two series, where the metal was casted in two beds of olivine sand, with approx. dimensions 1.3 x 1 x 0.3 m. In each bed subsequent layers were casted from the same ladle at subsequent taps of the furnace. In series 1 and 2 a total of five and four layers where made, with the thickness of each layer of approx. 40 and 60 mm, respectively. After completion of each test series, samples were taken from the centre of the metal plates and layers.

Results

Phase Relations in the System Mn - Fe - Si - C

In a previous paper [2] crystallization paths and phase compositions of commercial manganese alloys, with and without silicon, were discussed on the basis of calculated phase diagrams for the system Mn - Fe -Si - C. Thermodynamic properties of phases appearing in the six boundary binaries of this system were used as input data in these calculations, together with simplified solution models for the liquid phase and the solid solution phases that are known to exist in the Mn - Fe - Si ternary.

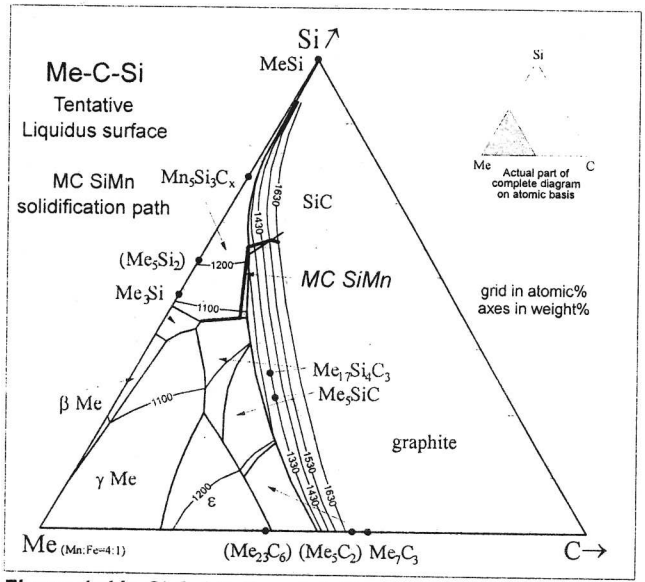

Figure 1: Me-Si-C, Mn:Fe = 4:1: Tentative liquidus surface; MC SiMn solidification path [1]. Graphite and SiC surfaces based on Tuset [3], others estimated or calculated by Termo-Calc [2].

The outcome of the calculations, which were in almost perfect agreement with accepted phase diagrams for the boundary binaries and published and obtained results on the system Mn - Fe - Si, disagreed when confronted with recent results on synthesized samples containing carbon [1]. The reason is that ternary/quaternary phases of the types $(Mn,Fe)_5SiC$ and '$(Mn,Fe)_8Si_2C$' are found to exist as stable phases in the C-containing systems. For the iron free compound of the latter phase two obtional formulas have been suggested in the litterature, namely $(Mn,Fe)_8Si_2C$ and $(Mn,Fe)_{17}Si_4C_3$.[5]. The present work indicates that the latter of the two appears to be closest to the actual composition of the '$(Mn,Fe)_8Si_2C$' phase, but the results are not sufficiently decisive for further refinement of the formula $(Mn,Fe)_{17}Si_4C_3$.

Based on the study of synthesized samples where 0, 10 and 20% of the manganese have been substituted by iron, tentative diagrams for the phase boundaries in the liquid surface of the system Me - Si - C (Me = Mn + Fe) has been derived [1]. The result for 20% Fe is presented in figure 1 showing also the location of the two ternary phases Me_5SiC and $Me_{17}Si_4C_3$.

Temperature Measurements

The temperature data from the chill casting series are shown for test #3 in figure 2, and cooling rate versus temperature for the full series in figure 3. The measurements start at approx. 1450 °C and ends below 600 °C. Evidently, the cooling rate varies greatly in this temperature range, from the initial high values through several local minima at ~1260 °C and in the range 1100-950 °C, and maxima between 1150-1100 and at ~900 °C, to a gradual decrease below 900 °C. The cooling rate is also dependant of the casting thickness, as it shifts towards lower values with thicker casts.

The temperature data from the layer casting series is shown for test series #2 in figure 4, and cooling rate versus temperature for both series in figure 5. The temperature measurements start at 1250 - 1350 °C

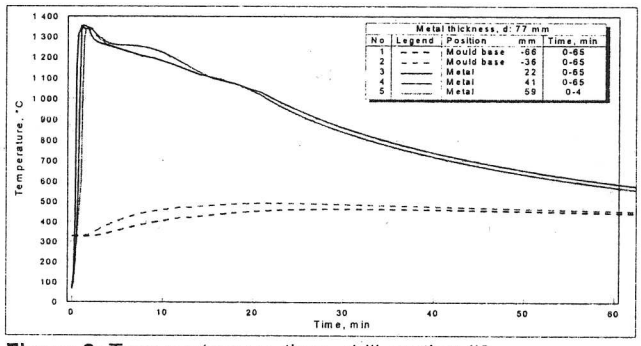

Figure 2: Temperature vs. time, chill casting #3.

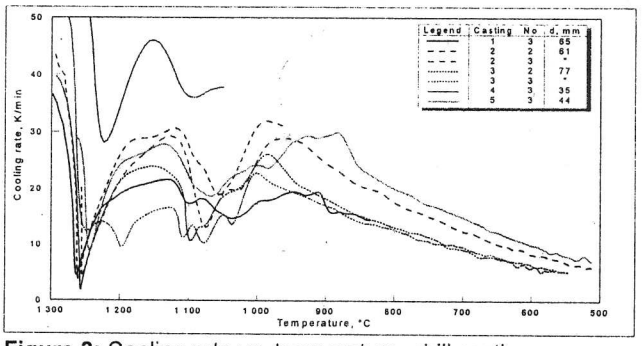

Figure 3: Cooling rate vs. temperature, chill casting.

and ends below 350 °C. In the same manner as seen for the chill casting, the cooling rate varies through the temperature range and with the casting thickness.

Macroscopic Examination

In all casts of commercial metal a distinct layer in the top 1/3 - 1/4 was observed. This region had a greyish shade compared to the 'metallic' glance of the lower part of the cast. Therefore the two parts were designated the 'carbide' and 'metal' regions, respectively, as shown schematically in figure 6. Vertical cut outs from each of the casts were devided in four, with partition numbering as given in the figure, each part was subsequently subjected to chemical analysis and microscopic examination.

Chemical Analysis

The partitioned samples of commercial metal were chemically analysed on Mn, Fe, Si, C, P, S, Ti and B, and the results are presented in figure 7 and table 1. For most elements the macrosegregation between the carbide and metal regions is evident, whereas they have relative stable values within the metal region. The contents of Si, C, S and Ti are increased in the carbide region, whereas Mn, Fe and B are showing decreased values. P does not vary significantly between the two regions.

Microscopic Examination

A selection of the commercial samples has been examined by electron microprobe (EPMA), which is a powerful tool to visualize compositional changes, as it gives qualitative and quantitative compositional information from narrow regions. Some of the acquired images are shown in figures 8 - 12.

Figure 8 shows the characteristic appearance of the carbide region. A large number of regular shaped inclusions are found scattered in this region, with a typical size of 50 - 100 μm. Figure 9 shows a close-up of a collection of these, from the differences in brightness it is evident that they separate in three different compositions. Element mapping (not included due to limited space) revealed that all particles contained more or less C, besides Si in the dark grey and Ti in the light grey ones. Hence, the particles are identified as graphite (black), SiC (dark grey) and TiC (light grey). For simplicity, they are refered to as carbon-based particles.

A different kind of inclusion is shown in Figure 10, found only in small numbers. Distinctive from the carbon-based particles, it is irregular in shape and of larger grain size (300 x 150 μm). Another notab-

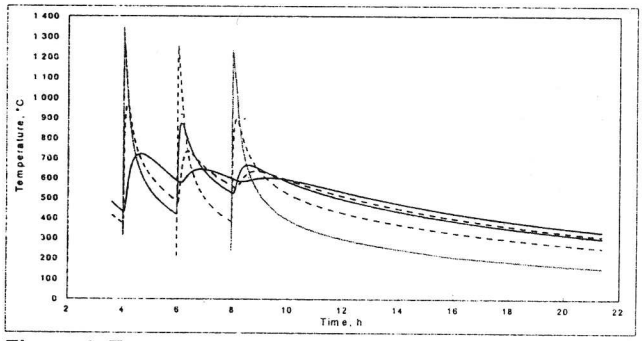

Figure 4: Temperature vs. time, layer casting #2.

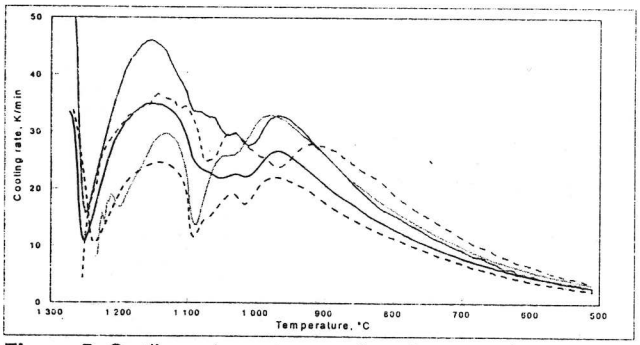

Figure 5: Cooling rate vs. temperature, layer casting.

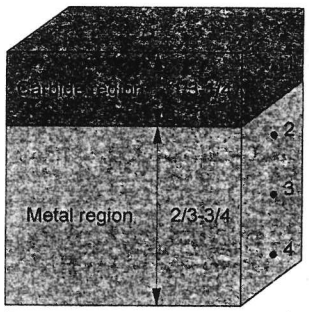

Figure 6: Carbide and metal regions in cast.

Table 1: Chemical analysis and macrosegregation in commercial samples.

Element	Vert. pos. 1	Vert. pos. 2-4	Rel. diff.%
Mn	67.4	70.7	-4.8
Fe	7.8	8.2	-4.4
Si	22.2	19.0	16
C	2.34	0.97	141
P	0.094	0.093	1.2
S	0.028	0.014	105
Ti	0.486	0.220	121
B	0.032	0.034	-5.7

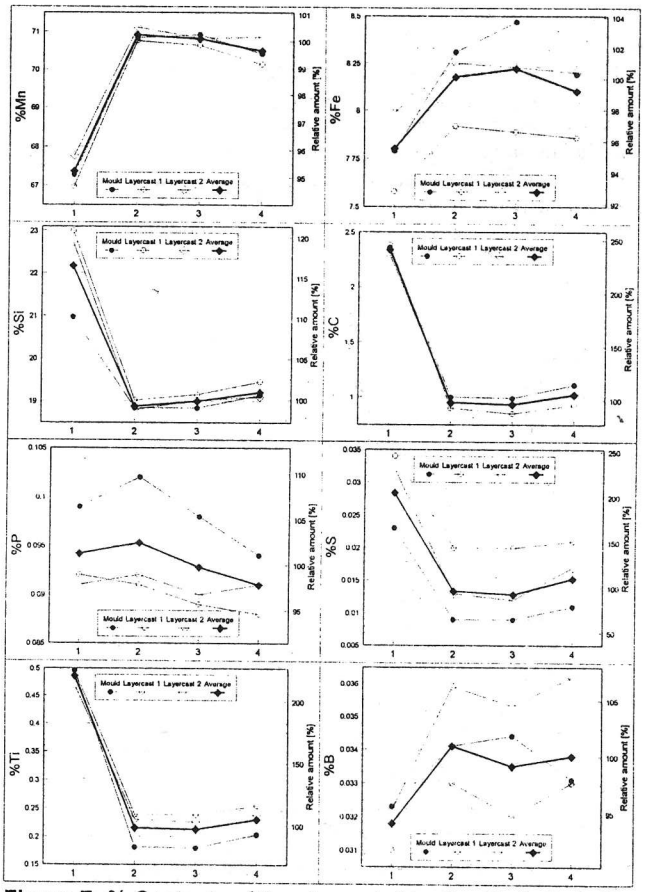

Figure 7: % Contents of the elements Mn, Fe, Si, C, P, S, Ti and B vs. vertical position (1, 2, 3, 4) in cast.

le feature is the large number of carbides sticking to or close to its surface. From its diversed brightness the inclusion is evidently a mixture of two phases, rather than a homogenous region, with the darker being predominant. Results of element mapping, given in table 2, show that the dark phase contains Mn, Si, O and some Al and Ca, whereas the light one contains Mn, S and O. 'Traces' of C and P are disregarded. Hence, the dark phase is most likely composed of $MnO{\cdot}SiO_2$($\cdot Al_2O_3$ $\cdot CaO$) and the light phase of $MnO{\cdot}MnS$. For simplicity, the whole particle is later called an oxidic inclusion.

Figure 11 shows the appearance of the metal region, which is without visible particles or inclusions. However, from its diversed brightness the region evidently separates in three different compositions, readily apparent in the close-up in figure 12, with the darkest phase being predominant. Results of microanalysis given in table 3, reveal large differences in the composition of the three phases. Besides the main elements Mn, Fe and Si, the minor elements Ti and P have been traced, whereas B and C are below the detection limit for quantitative analysis. By area fraction measurement the dark, grey and light phase count for approx. 70, 25 and 5% by weight, respectively.

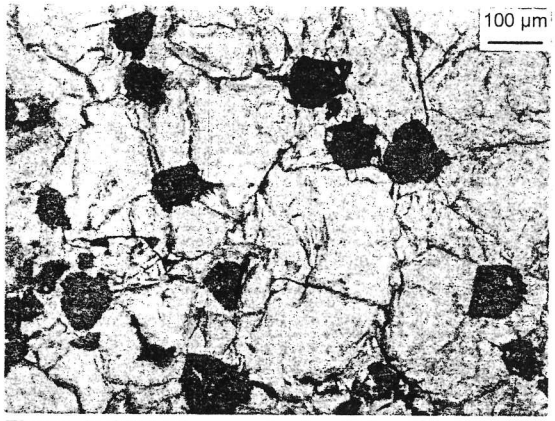

Figure 8: SEM Micrograph of carbide region. 100X

Figure 9: Close-up on carbide particles. 1000X

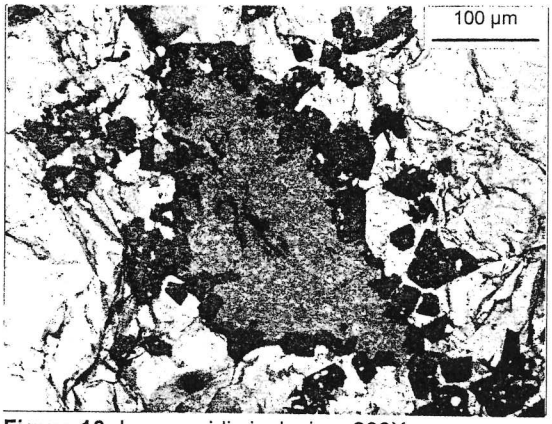

Figure 10: Large oxidic inclusion. 200X

Table 2: Element mapping of irregular inclusion.

Element	Phase	
	Light	Dark
Mn	Very high	High
Fe	None	None
Si	Very low	Moderate
C	Very low	Very low
Ti	None	None
P	Low	Low
S	High	None
O	Moderate	High
N	None	None
Al	None	Low
Ca	None	Very low
Mg	None	None

Table 3: Microanalysis (w%) and weight fraction of metallic phases in cast.

Element	Phase		
	Light	Grey	Dark
Mn	70.9	78.3	67.5
Fe	13.2	8.2	8.8
Si	13.7	8.4	20.6
Ti	0.05	0.06	0.21
P	0.40	0.03	0.06
Sum	98.2	95.0	97.2
wf,%	~5	~25	~70

Table 4: Chemical analysis of potential compounds (w%).

Name	Me[1]	Si	C
Me_5Si_3[2]	76.0	23.3	0.73
$Me_{17}Si_4C_3$	86.1	10.5	3.33
Me_3Si	85.4	14.6	-[3]
Mn_5Si_2	83.0	17.0	-[3]

[1]Me = Mn + Fe, Fe substitutes Mn.
[2]Solubility of C up to $C_{0.22}$. [4]
[3]Solubility of C unknown.

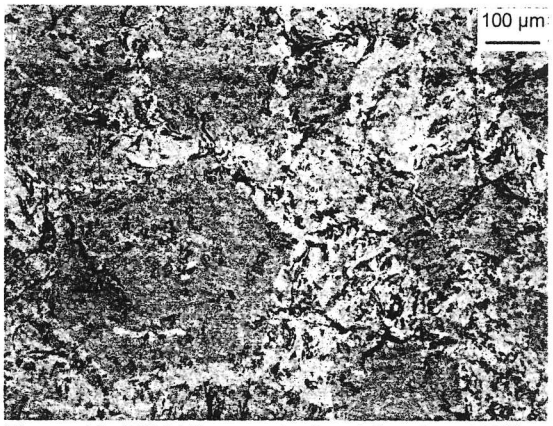

Figure 11: SEM Micrograph of metal region. 100X

Figure 12: Close-up of metal phases. 1000X

The phases are identified from their contents of Mn+Fe and Si, see table 4 for reference to their actual composition, while the contents of Ti and P have been disregarded in this context. Hence, the phases are designated Me_5Si_3 (dark), $M_{17}Si_4C_3$ (grey) and Me_5Si_2 (light).The agreement with the actual compositions is quite good, although the Si values in general are somewhat too low.

X-ray Diffraction

The synthesized samples and a selection of the commercial samples have been investigated by the powder method for x-ray diffraction (XRD). Due to limited space, the XRD diagrams for the synthesized samples are omitted in this presentation, only a selection of the commercial samples are given.

Figure 13 shows the X-ray diffractograms of three samples from the carbide region as compared with the reference patterns of Mn_5Si_3, $Mn_{22.4}Si_{5.6}C_4$ ($Mn_{17}Si_4C_3$), Mn_5Si_2, SiC and graphite. A very good correlation with the former two is seen, which are the primary and secondary metal phases. Due to low amounts of the third metal phase and the two carbon-based phases, just a few week lines that match the reference patterns of the remaining three are seen, especially for Mn_5Si_2 and graphite. Some lines are left unresolved, as they can not be fitted to any relevant reference pattern with reasonable certainty. They may be associated with oxidic inclusions.

Figure 14 shows the X-ray diffractograms of three samples from the metal region as compared with the reference patterns of Mn_5Si_3, $Mn_{22.4}Si_{5.6}C_4$ and Mn_5Si_2. Again, a very good correlation with reference pattern for the primary and secondary metal phases is seen, but also the reference pattern for the third metal phase is in this case quite satisfactory matched. Fewer lines are left unresolved, which is reasonable as no other phases have been seen in the metal region.

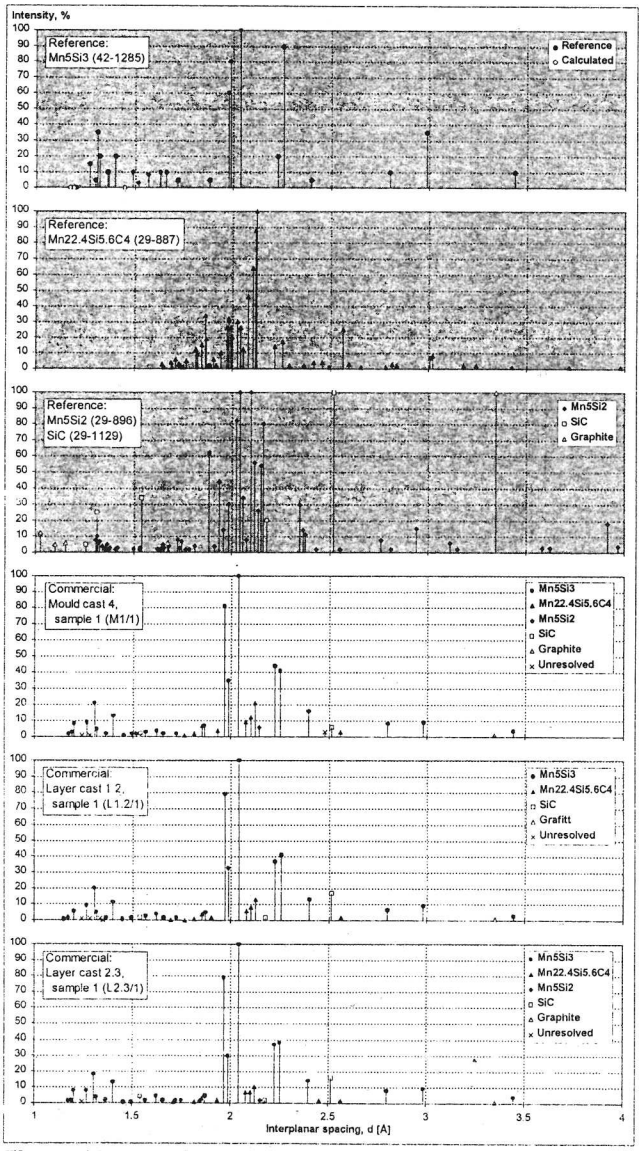

Figure 13: Matching of XRD-patterns of carbide region.

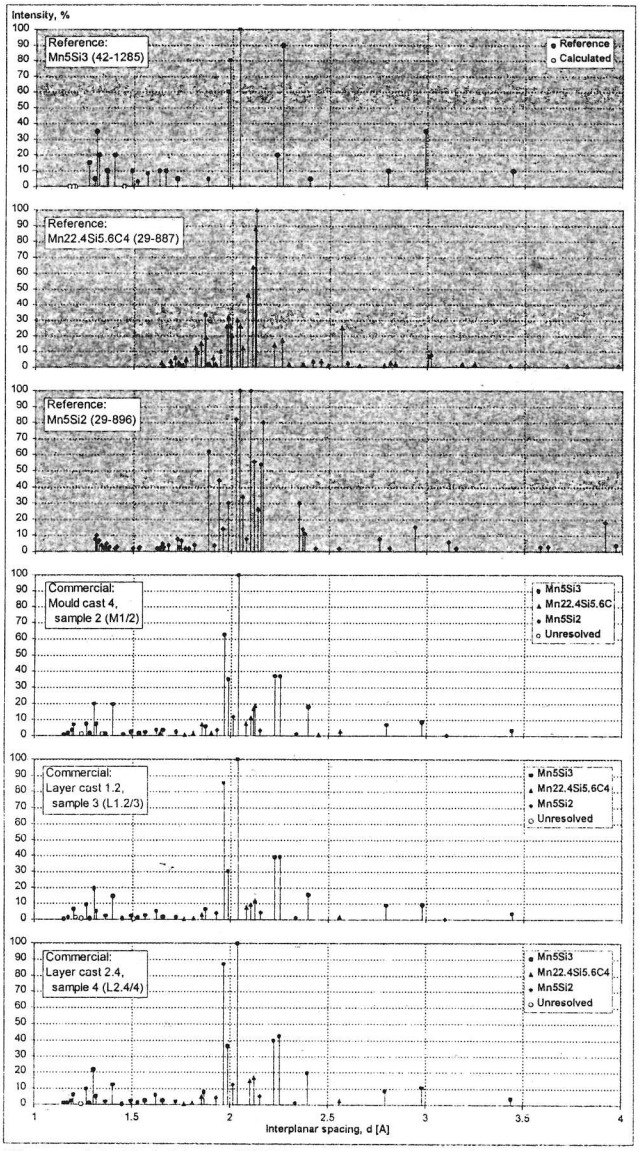

Figure 14: Matching of XRD-patterns of metal region.

Hardness measurements

Micro hardness measurements made on synthesized samples have revealed that the major phases are brittle, with Vickers hardness numbers of 826 and 946 for Me_5Si_3 and Me_8Si_2C, respectively, accompanied with extensive cracking for both. The third metal phase, if present as Me_3Si, is somewhat more ductile, with a Vickers hardness number of 646 and no cracking. It has not been established how the solid state transformation to Me_5Si_2 influences the strength.

From tumbler testing of commercial SiMn it is found that large grained metal is more fragile than the small grained material. Hence, the strength of the alloy is improved by rapid solidification.

Discussion

The progress of solidification can be evaluated from the recorded cooling rates given in figure 3 and 5. There is a minimum in the cooling rate at ~1260 °C that reflects the onset of the primary formation of the Me_5Si_3-phase after the initial precipitation of SiC in figure 1 where a probable crystallization path is indicated. The next minimum in the cooling rate appears at ~1100 °C and reflects that the second phase $Me_{17}Si_4C_3$ starts to coprecipitate with the primary phase. Finally the minima between 1100 and 1000 °C represent the eutectic reaction where the solidification prosess ends with the formation of the third phase Me_3Si. This phase however, has not been detected in the x-ray diffractograms, but so has Mn_5Si_2, a phase which is not formed directly from the melt. Thus, a solid state reaction of the type: 1/4 Mn_5Si_3 + 5/4 Me_3Si = Me_5Si_2 must have taken place, as seen at around 900 °C for two of the cooling rate curves in figure 3.

Acknowledgement

This work has been financially supported by The Norwegian Ferroalloy Producers Research Association (FFF) and The Research Council of Norway (NFR). Elkem Mangan Sauda has supported its completion. They are all greatly acknowledged.

References

[1] Hoel, Eivind G.: *Structure and Phase Relations of MC SiMn*, Doctoral Thesis, NTNU, *to be published.*

[2] Hoel, Eivind G.: *Phase Relations of Mn-Fe-Si-C Systems*, INFACON 7, 601, 1995.

[3] Tuset, J. Kr.; Sandvik, J.: *The Solubility of Carbon in Ferrosilicomanganese at 1330 - 1630 °C*, SINTEF-report, Project 2268 340358, 1970.

[4] J.-P. Senateur et al., *Influences of non stoichiometry on the magnetic properties of the Mn_3GaC_{1-x} and $Mn_5Si_3C_x$ phases*, Bull. Soc. fr. Minéral. Cristallogr., 1967, XC, 537-543.

[5] P. Spinat et al., *Structural Study of the 'Mn_8Si_2C' Phase*, Acta Cryst. (1975). B31, 541-7.